A fast algorithm for computing dynamic tyre road contact forces

Denis Duhamel, Rabie Meftah, Julien Cesbron, Yin Hai-Ping

ACOUSTICS 2012

A fast algorithm for computing dynamic tyre road contact forces

D. Duhamel[a], R. Meftah[a], J. Cesbron[b] and H.-P. Yin[a]

[a]Université Paris-Est - UMR Navier, Ecole des Ponts ParisTech, 6&8 av. Blaise Pascal - Champs-sur-Marne, 77455 Marne La Vallée Cedex 2, France
[b]LUNAM Université, IFSTTAR, IM, EASE, Route de Bouaye, 44344 Bouguenais, France
denis.duhamel@enpc.fr

Tire/road contact is the principal source of car noise at speeds greater than 50 km/h. In this context, we have developed a new approach for modelling the tire vibrations and the contact with the rigid road surfaces during rolling. For the tire, a periodic model is used to compute Green's functions. The response of the tire can thus be modelled over a large frequency range. Then a fast convolution and contact model is developed and examples of computations of contact forces are given for real road textures. Spectra of forces for different tire velocities are also computed.

1 Introduction

The computation of tire road noise needs first a model for the tire vibration and then a method for computing contact forces between a tire and a road. For the tire vibrations, the simplest approach is the circular ring model as in [1]. However for complex geometrical or material properties of the tire a finite element model is much more appropriate. To avoid the heavy three-dimensional computations of [2], several efficient models have been proposed such as the wave finite element approach in [3] or the recursive method presented in [4, 5].

Here the dynamic response of the tire is calculated by convolution of the contact forces with the Green's functions of the tire. For orthotropic plates such Green's functions were analytically found in [6], but here they are found from the recursive model [4]. However the computation of the convolution can be time consuming. In this work we have used a new method. First it consists in the modal expansion of the pre-calculated Green's functions. The modal parameters are then used to construct a new convolution which allows quicker calculations than the traditional convolution. The modal convolution is adapted to dynamic contact problems by using a kinematic contact condition. The outline of the paper is thus the following. In section 2, the tire model is first presented. Then in section 3, the contact model, including the fast convolution and the kinematic contact condition is described. Finally, section 4 gives numerical results of displacements and contact forces for two road textures.

2 Tire model

2.1 Tire section

The first step is to have a model for the vibrations of the tire. Here a periodic model has been developed. It consists in modelling a short cell of the tire as in Figure 1 and using calculations on this cell for computing Green's functions as described below. Stiffness and mass matrices of a cell are obtained from commercial finite element software. In a first step they are obtained in a cartesian coordinate system and then they are transformed in a cylindrical coordinate system in which the whole structure is periodic.

The tire is also inflated with an internal pressure P. So its vibrations are considered as a small perturbation of the prestressed static state shown in Figure 1. This prestress generates an additional stiffness matrix denoted K_P. So, the full dynamic stiffness matrix is given by:

$$\mathbf{D}(\omega) = \left[\mathbf{K} + \mathbf{K}_P + j\omega\mathbf{C} - \omega^2\mathbf{M}\right] \tag{1}$$

The tire studied here is of type Michelin 165/65/R13 77T. Its geometric properties are given in Table 1. The mechanical properties of the different parts of the tire are given in Table 2.

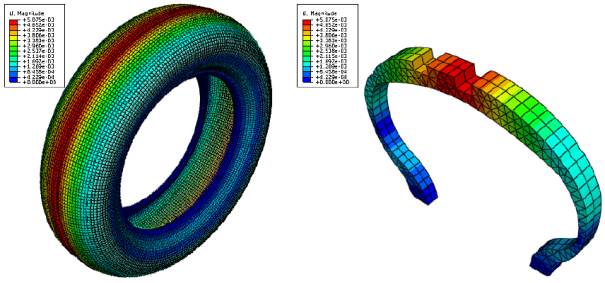

Figure 1: Section of the tire and displacements for an inflation pressure of 2 $bars$.

Internal diameter	13" (330.2 mm)
Width of the tread	165 mm
Height of the sidewall	65 mm

Table 1: Properties of tire Michelin 165/65/R13 77T.

Part	Material	Property	Value
Tread pattern	Rubber	ρ E ν	1000 kg/m^3 7 MPa 0,49
Bead	Steel	ρ E ν	7850 kg/m^3 162, 6 GPa 0,33
Sidewall	Rubber +nylon belt	ρ E ν	1000 kg/m^3 109 MPa 0, 48
Tread	Rubber +steel belt	ρ E_r E_x ν_{ry} G_{ry}	2014 kg/m^3 663 MPa 624 MPa 0,4 330 MPa

Table 2: Mechanical properties of the tire.

2.2 Equivalent matrix

The aim of the periodic model is to built the global dynamic stiffness matrix of the structure from the dynamic stiffness matrix of a single period. It is obtained by recursively eliminating the internal degrees of freedom between adjacent cells. Consider the dynamic stiffness matrices $\mathbf{D}^1$ and $\mathbf{D}^2$ of two neighbouring cells:

$$\mathbf{D}^1 = \begin{bmatrix} \mathbf{D}^1_{LL} & \mathbf{D}^1_{LR} \\ \mathbf{D}^1_{RL} & \mathbf{D}^1_{RR} \end{bmatrix} \; ; \; \mathbf{D}^2 = \begin{bmatrix} \mathbf{D}^2_{LL} & \mathbf{D}^2_{LR} \\ \mathbf{D}^2_{RL} & \mathbf{D}^2_{RR} \end{bmatrix} \tag{2}$$

The equivalent matrix of the two cells structure is obtained by eliminating the internal degrees of freedom by:

$$\mathbf{D}^{eq} = \begin{bmatrix} \mathbf{D}^1_{LL} - \mathbf{D}^1_{LR}\mathbf{D}^*\mathbf{D}^1_{RL} & -\mathbf{D}^1_{LR}\mathbf{D}^*\mathbf{D}^2_{LR} \\ -\mathbf{D}^2_{RL}\mathbf{D}^*\mathbf{D}^1_{RL} & \mathbf{D}^2_{RR} - \mathbf{D}^2_{RL}\mathbf{D}^*\mathbf{D}^2_{LR} \end{bmatrix} \quad (3)$$

with:

$$\mathbf{D}^* = \left[\mathbf{D}^1_{RR} + \mathbf{D}^2_{LL}\right]^{-1}$$

This operation is repeated n times with n such that:

$$N = \sum_{i=1}^{n} 2^{p_i} \;\; ; \;\; p_1 > p_2 ... > p_n \quad (4)$$

with p_i the position of the i^{th} figure in the binary representation of the number N of cells in the tire.

2.3 Green's functions

Consider the domain Ω of the tire. It can be separated into two subdomains Ω_l et Ω_c. The number of cells in the domain Ω_c where the contact occurs, is denoted by N_c. The other free part Ω_l of the tire has N_l cells, see Figures 2 and 3.

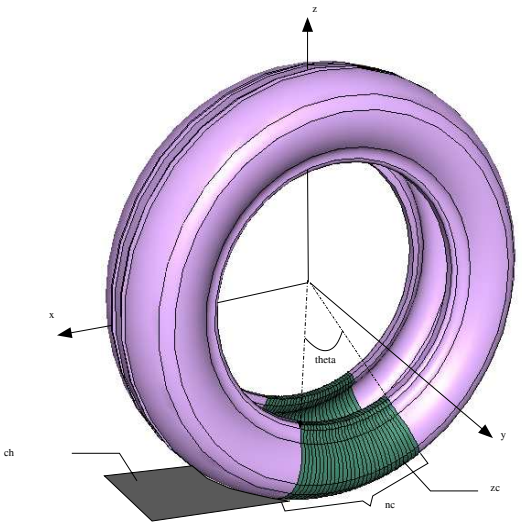

Figure 2: Contact zone with the road.

The dynamic stiffness matrix of domain Ω_l, denoted $\mathbf{D}^{eq}$, is computed by the method presented in section 2.2. Then the full dynamic stiffness matrix of the tire is computed by a standard finite element assembling between $\mathbf{D}^{eq}$ and the matrices of the N_c cells of Ω_c, see Figure 3 and Eq. (5). The matrix of Green's functions is obtained by solving a linear system with Eq. (5) and different load cases associated to different points in the contact zone. The number of load cases is limited to the number of dofs in a section of the tire.

$$\underbrace{\begin{bmatrix} \mathbf{D}_{11} + \mathbf{D}^{eq}_{11} & \mathbf{D}_{12} & \mathbf{0} & \dots & \mathbf{D}^{eq}_{12} \\ \mathbf{D}_{21} & \mathbf{D}_{22} + \mathbf{D}_{11} & \ddots & \ddots & \ddots \\ \mathbf{0} & \ddots & \ddots & \ddots & \ddots \\ \vdots & \ddots & \ddots & \mathbf{D}_{11} + \mathbf{D}_{22} & \mathbf{D}_{12} \\ \mathbf{D}^{eq}_{21} & \ddots & \ddots & \mathbf{D}_{21} & \mathbf{D}_{22} + \mathbf{D}^{eq}_{22} \end{bmatrix}}_{\mathbf{D}_T} \quad (5)$$

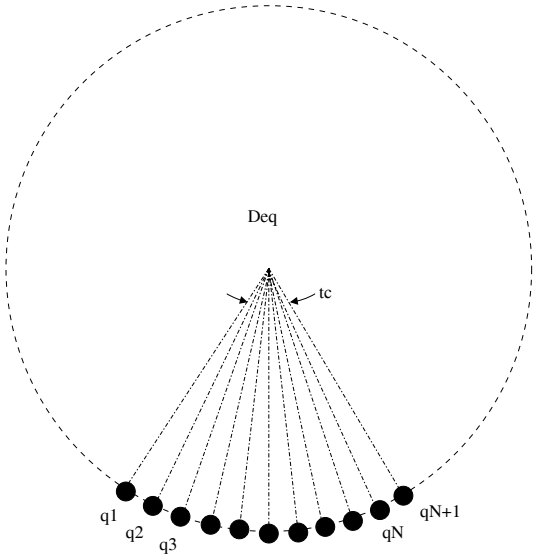

Figure 3: Dofs of the global matrix.

3 Contact model

3.1 Fast convolution

The computation of the response of the tire by a standard convolution requires a large number of coefficients. Here we try to reduce the computing time by simplifying the Green's function which can be approximated by a linear combination of modes (not necessarily the true modes) as:

$$G(\omega) = \sum_{k=1}^{k=N_m} \frac{A_k}{-\omega^2 + 2j\xi_k\omega\omega_k + \omega_k^2} \quad (6)$$

Knowing $G(\omega)$ by a finite element model or by measurements, we must identify the residues A_k, the dampings ξ_k and the resonance frequencies ω_k. There are several methods to solve this problem. In this study the LSCE (Least Squares Complex Exponential) is used.

The Green's function of the tire is first computed with the periodic model, then the modal parameters are identified by the precedent method. For each coefficient of the Green's matrix an optimal number of coefficient N_m is chosen to get the best approximation. The error is low, generally below 5%. In Figure 4, a Green's function and its approximation are presented for the coefficient with the maximal error (6.5%). One can see that the approximation is very good.

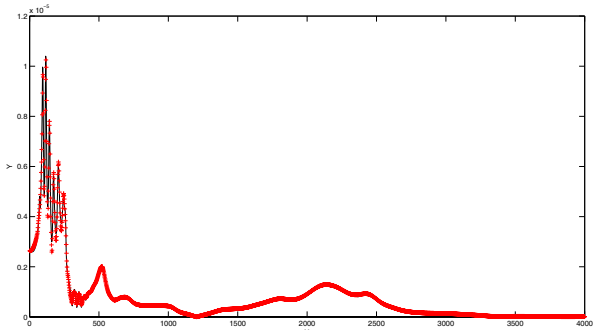

Figure 4: Comparison between a Green's function ─ and its approximation -+- in the least favourable case.

By taking the inverse Fourrier transform, the Green's function in the time domain can be found by:

$$g(t) = \sum_{k=1}^{k=N_m} \frac{A_k}{\omega_k^d} e^{-\xi_k \omega_k t} sin(\omega_k^d\ t) H(t) \tag{7}$$

with:

$$\omega_d^k = \omega_k \sqrt{1 - \xi_k^2}$$

The displacement $u(t)$ is obtained from the contact force $q(t)$ by the convolution:

$$u(t) = \int_0^t\ g(\tau) q(t-\tau) d\tau = \int_0^t\ g(t-\tau) q(\tau) d\tau \tag{8}$$

Inserting the expression (7) for $g(t)$ in Eq. (8) yields:

$$u(t) = \int_0^t \sum_{k=1}^{k=N_m} \frac{A_k}{\omega_k^d} e^{-\xi_k \omega_k\ (t-\tau)} sin\left(\omega_k^d\ (t-\tau)\right) q(\tau) d\tau \tag{9}$$

Separating the t and τ variables and rearranging, the displacement can be written as:

$$u(t) = \sum_{k=1}^{k=N_m} \frac{A_k}{\omega_k^d} e^{-\xi_k \omega_k t} \left[sin\left(\omega_k^d\ t\right) \alpha^k(t) - cos\left(\omega_k^d\ t\right) \beta^k(t) \right] \tag{10}$$

where $\alpha^k(t)$ and $\beta^k(t)$ are computed by:

$$\begin{aligned} \alpha^k(t) &= \int_0^t\ e^{\xi_k \omega_k \tau} cos(\omega_k^d\ \tau) q(\tau) d\tau \\ \beta^k(t) &= \int_0^t\ e^{\xi_k \omega_k \tau} sin(\omega_k^d\ \tau) q(\tau) d\tau \end{aligned} \tag{11}$$

The parameters $\alpha_k(t + \Delta t)$ and $\beta_k(t + \Delta t)$ can be computed by the discrete versions of Eq. (11) as:

$$\begin{aligned} \alpha^k((n+1)\Delta t) &= \alpha^k(n\Delta t) + e^{\xi_k \omega_k n \Delta t} cos(\omega_k^d\ n\Delta t) q(n\Delta t) \Delta t \\ \beta^k((n+1)\Delta t) &= \beta^k(n\Delta t) + e^{\xi_k \omega_k n \Delta t} sin(\omega_k^d\ n\Delta t) q(n\Delta t) \Delta t \end{aligned} \tag{12}$$

3.2 Kinematic contact conditions

When there is no contact, the contact force equals zero and the displacement can be computed by the fast convolution. When there is contact, conditions must be written to find the contact force. We propose here to write two conditions, one for the displacement and the other for the velocity.

Eq. (8) can be separated into a term depending on the past history of forces $u_h(t)$ and another term depending only on the present time step:

$$u(t) = \underbrace{\int_0^{t-\Delta t} g(t-\tau) q(\tau) d\tau}_{u_h(t)} + \int_0^{\Delta t}\ g(\tau) q(t-\tau) d\tau \tag{13}$$

In the same way taking the derivative of Eq. (13) leads to an equation in term of the velocity:

$$v(t) = \underbrace{\int_0^{t-\Delta t} g'(t-\tau) q(\tau) d\tau}_{v_h(t)} + \int_0^{\Delta t}\ g'(\tau) q(t-\tau) d\tau \tag{14}$$

Denoting $\mathbf{Y} = [u(t)\ \ v(t)]^T$ and $\mathbf{Y}_h = [u_h(t)\ \ v_h(t)]^T$ leads to:

$$\mathbf{Y} = \mathbf{Y}_h + \Psi(q) \tag{15}$$

where Ψ is an integral operator giving the influence of the contact force at present time on the displacement and the velocity. So the contact conditions are:

$$\mathbf{Y} = \mathbf{Y}_r = [u_r(t)\ \frac{du_r(t)}{dt}]^T \tag{16}$$

where $u_r(t)$ and $\frac{du_r(t)}{dt}$ are the position of the road and its velocity as seen in the tire reference system. Using the modal decompositions for the displacement and the velocity yields:

$$u(t) = \sum_{k=1}^{k=N} \frac{A_k}{\omega_k^d} e^{-\xi_k \omega_k t} \left[sin\left(\omega_k^d\ t\right) \alpha^k(t) - cos\left(\omega_k^d\ t\right) \beta^k(t) \right] \tag{17}$$

and

$$\begin{aligned} v(t) \quad = \quad & -\sum_{k=1}^{k=N} \frac{A_k \xi_k \omega_k}{\omega_k^d} e^{-\xi_k \omega_k t} \left[sin\left(\omega_k^d\ t\right) \alpha^k(t) - cos\left(\omega_k^d\ t\right) \beta^k(t) \right] \\ & + \sum_{k=1}^{k=N} A_k e^{-\xi_k \omega_k t} \left[cos\left(\omega_k^d\ t\right) \alpha^k(t) + sin\left(\omega_k^d\ t\right) \beta^k(t) \right] \end{aligned} \tag{18}$$

The $u^h(t)$ and $v^h(t)$ values are obtained from Eq. (17) and (18) by computing α and β with $q = 0$ at the present time. The real value of this force $q(t)$ at present time is such that:

$$\begin{aligned} \Delta\mathbf{Y} \quad &= \quad \mathbf{Y}_r - \mathbf{Y}^h \\ &= \quad \begin{bmatrix} \int_0^{\Delta t}\ g(\tau) q(t-\tau) d\tau \\ \\ \int_0^{\Delta t}\ g'(\tau) q(t-\tau) d\tau \end{bmatrix} \end{aligned}$$

The integrals can be computed by Gauss quadratures with two points. The values of the forces at these two Gauss points are obtained by:

$$\mathbf{q} = \begin{bmatrix} q_1 \\ q_2 \end{bmatrix} = \Psi^{-1}(t_1, t_2) \Delta\mathbf{Y} \tag{19}$$

with Ψ defined by:

$$\Psi = \begin{bmatrix} g(t_1) & g(t_2) \\ \\ g'(t_1) & g'(t_2) \end{bmatrix} \frac{\Delta t}{2} \tag{20}$$

and

$$\begin{aligned} t_1 \quad &= \quad t + \left(1 - \frac{1}{\sqrt{(3)}}\right) \frac{\Delta t}{2} \\ t_2 \quad &= \quad t + \left(1 + \frac{1}{\sqrt{(3)}}\right) \frac{\Delta t}{2} \end{aligned} \tag{21}$$

From the knowledge of the contact forces at times t_1 and t_2, the parameters $\alpha_k(t + \Delta t)$ and $\beta_k(t + \Delta t)$ can be computed by Eq. (12). This method can be easily generalised for a surface with several contact points. In this case the number of contact points can change with time. The contact occurs when $u^h(t) \leq u_r(t)$ for each point in the contact zone. Then the generalization of Eq. (16) for the points where the contact happens allows to determine the contact forces at these points.

4 Road contact

4.1 Road texture

We assume that the roads are perfectly rigid and that the contact area is constant with time. We consider two road textures obtained during the French-German project DEUFRAKO P2RN. The measured area is $L = 2m$ long and $b = 0.35m$ width with a sampling of $dx = dy = 384\ \mu m$. Figure 5 presents the samples of two different roads of sizes 0.1 m by 0.1 m, see [7] for other examples.

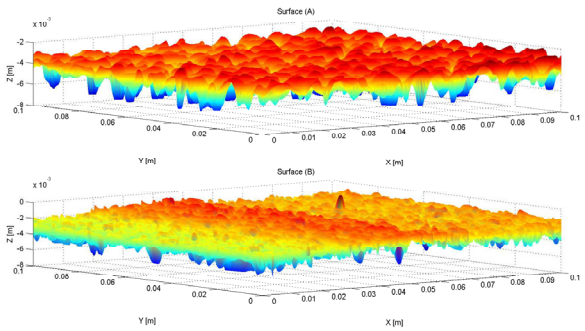

Figure 5: $3D$ texture of the two roads: (A) upper figure and (B) lower figure.

We want to compute the displacements and forces in the contact zones. The Green's functions of the tire are computed as in section 2 in the frequency range [0 4000 Hz]. The contact zone is changing as the tire is moving during the rolling process. The contact points are moving in the fixed coordinate system as:

$$\begin{aligned} x &= x_0 + V_0 t \\ y &= y_0 \\ z &= u_r(x, y) \end{aligned} \tag{22}$$

where (x_0, y_0, z_0) are the coordinates in the system moving at constant velocity V_0 with the tire. The maximal contact area is constant with time while the real contact area and the number of contact points can change.

4.2 Numerical results

All the simulations are made for a contact length $L_c = 6\ cm$ and a width $l_c = 8\ cm$. The number of points is $N_x = 10$ along X and $N_y = 12$ along Y. The tire is rolling over a length of $L = 2m$. The tread is discretized with steps of $dX \approx dY \approx 5\ mm$ with an interpolation of the tire height between two tread points. Figures 6 and 7 present the displacements and forces for the two road surfaces of Figure 5. The displacements have shapes similar to road textures. Losses of contact and high forces are seen at the maximal heights of asperities. Road (A) generates higher forces than road (B).

The force level, denoted L_f and computed in decibels relatively to a reference value of $F_c^0 = 10^{-4} N$, is obtained by:

$$L_f = 20 \log_{10} \left(\frac{|F_c(\omega)|}{F_c^0} \right) \tag{23}$$

Figures 8 and 9 present the third octave force spectra for roads (A) and (B) and for different velocities. When the velocity increases the spectra are shifted towards higher frequencies and the maximal level is also increased. The force

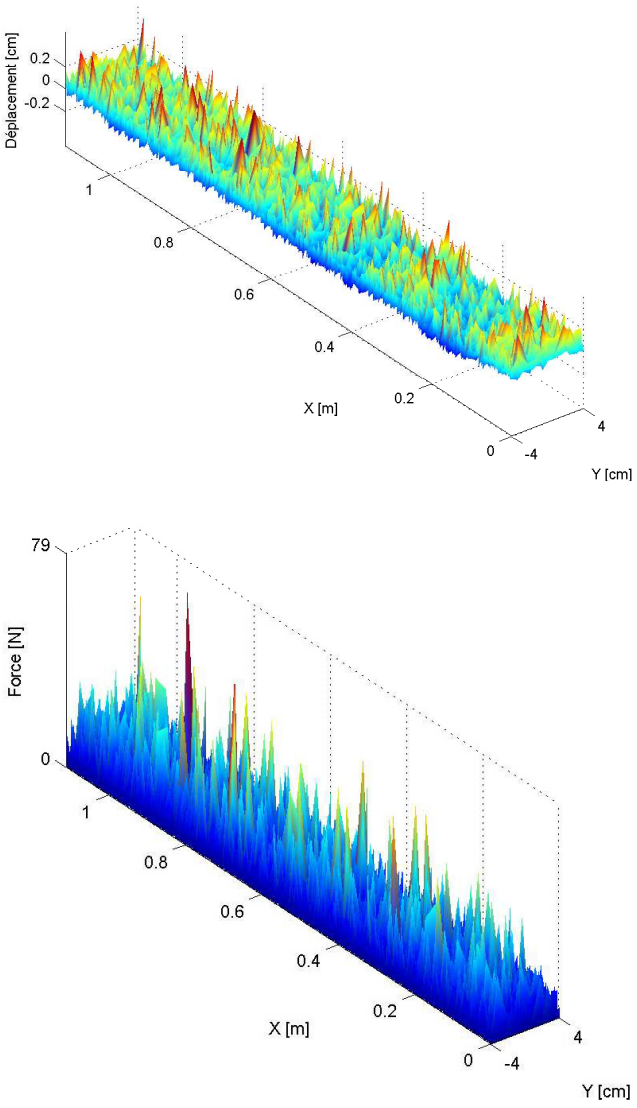

Figure 6: Displacements and forces for road (A) and for points such that $x_0 = 0$ with $V_0 = 90\ km/h$.

level is quite significant for frequencies between 500 Hz and 5000 Hz. For road (A) the maximum level is obtained for 4000 Hz, while for road (B) it is for 2000 Hz. Globally the force level is higher for road (A) than for road (B). More examples can be found in [8].

5 Conclusion

The periodic tire model allows to compute tire vibrations in a contact zone of size 6×8 cm^2 with 120 points over a large frequency range. The displacements and forces are obtained for a road length of $L = 2m$ and for two road surfaces. Results show that the force levels are highly dependant on the texture levels and the tire velocities. Increasing the tire velocity clearly shifts the force levels towards higher frequencies and increases the global level. Force levels are also significant between 500 Hz and 5000 Hz.

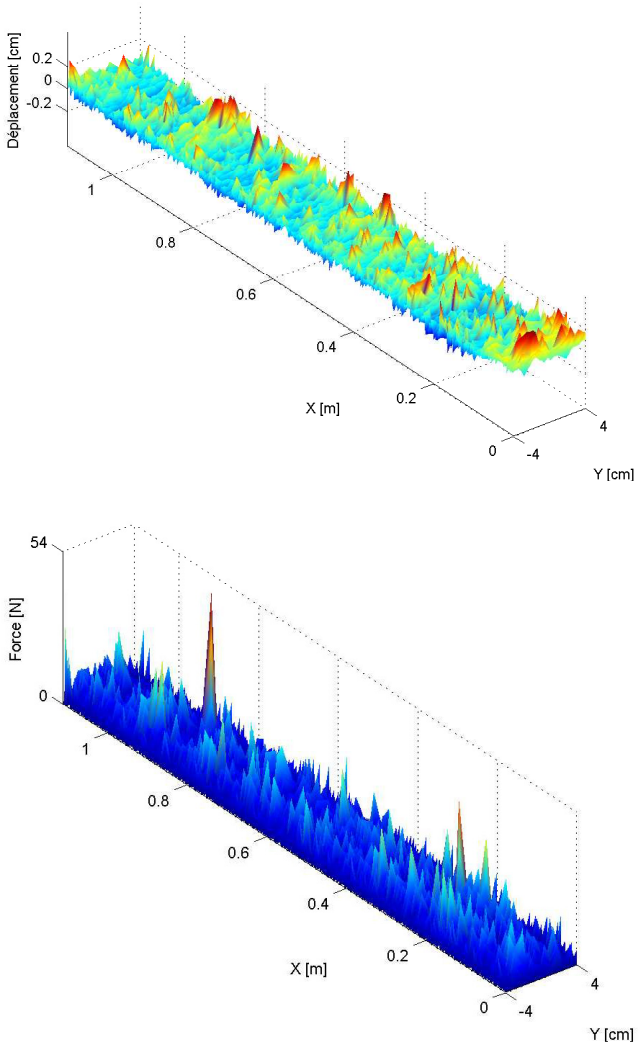

Figure 7: Displacements and forces for road (B) and for points such that $x_0 = 0$ with $V_0 = 90\ km/h$.

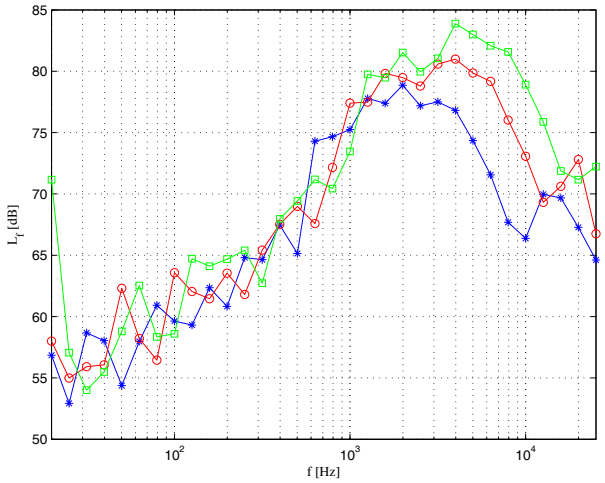

Figure 8: Third octave spectrum of the contact force at point $(x_0 = 0, y_0 = 0)$ for road (A) and for the velocities: -*- $V_0 = 50\ km/h$, -o- $V_0 = 70\ km/h$, -□- $V_0 = 90\ km/h$.

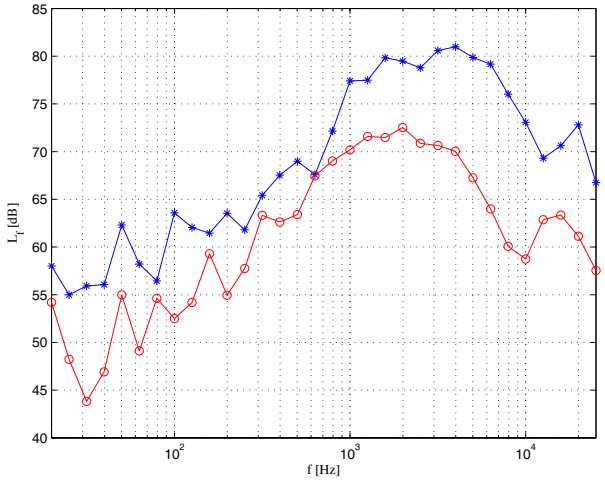

Figure 9: Third octave spectrum of the contact force at point $(x_0 = 0, y_0 = 0)$ for: -*- road (A),-o- road (B).

References

[1] S.C. Huang and W. Soedel. Response of rotating rings to harmonic and periodic loading and comparison with the inverted problem. *Journal of Sound and Vibration*, 118(2):253–270, 1987.

[2] M. Brinkmeier, U. Nackenhorst, S. Petersen, and O. von-Estorff. A finite element approach for the simulation of tire rolling noise. *Journal of Sound and Vibration*, 309:20–39, 2008.

[3] Y. Waki, B.R. Mace, and M.J. Brennan. Free and forced vibrations of a tyre using a wave/finite element approach. *Journal of Sound and Vibration*, 323:737–756, 2009.

[4] D. Duhamel. A recursive approach for the finite element computation of waveguides. *Journal of Sound and Vibration*, 323(1-2):163–172, 2009.

[5] D. Duhamel, S. Erlicher, and H.H. Nguyen. A recursive finite element method for computing tyre vibrations. *European Journal of Computational Mechanics*, 20(1-4):9–27, 2011.

[6] J. F. Hamet. Tire/road noise: time domain green's function for the orthotropic plate model. *Acta acoustica united with Acustica*, 87:470–474, 2001.

[7] Prediction and propagation of rolling noise. Technical report, Deufrako P2RN project, March 2009.

[8] R. Meftah. *Une approche par formalisme de Green réduit pour le calcul des structures en contact dynamique: application au contact pneumatique chaussée*. PhD thesis, Université Paris-Est, 2011.